

Weak measurements of a large spin angular splitting of light beam on reflection at the Brewster angle

Xinxing Zhou, Hailu Luo*, and Shuangchun Wen[†]

Key Laboratory for Micro-/Nano-Optoelectronic Devices of Ministry of Education, College of Information Science and Engineering, Hunan University, Changsha 410082, People's Republic of China

[†]scwen@vip.sina.com

[*hailuluo@hnu.edu.cn](mailto:hailuluo@hnu.edu.cn)

Abstract: We reveal a large spin angular splitting of light beam on reflection at the Brewster angle both theoretically and experimentally. A simple weak measurements system manifesting itself for the built-in post-selection technique is proposed to explore this angular splitting. Remarkably, the directions of the spin accumulations can be switched by adjusting the initial handedness of polarization.

© 2018 Optical Society of America

OCIS codes: (240.3695) Linear and nonlinear light scattering from surfaces; (260.5430) Polarization; (240.0240) Optics at surfaces.

References and links

1. M. Onoda, S. Murakami, and N. Nagaosa, "Hall effect of light," *Phys. Rev. Lett.* **93**(8), 083901 (2004).
2. K. Y. Bliokh and Y. P. Bliokh, "Conservation of angular momentum, transverse shift, and spin Hall effect in Reflection and Refraction of an Electromagnetic Wave Packet," *Phys. Rev. Lett.* **96**(7), 073903 (2006).
3. O. Hosten and P. Kwiat, "Observation of the spin Hall effect of light via weak measurements," *Science* **319**(5864), 787-790 (2008).
4. Y. Qin, Y. Li, H. He, and Q. Gong, "Measurement of spin Hall effect of reflected light," *Opt. Lett.* **34**(17), 2551-2553 (2009).
5. A. Aiello and J. P. Woerdman, "Role of beam propagation in Goos-Hänchen and Imbert-Fedorov shifts," *Opt. Lett.* **33**(13), 1437-1439 (2008).
6. J.-M. Ménard, A. E. Mattachione, M. Betz, and H. M. van Driel, "Imaging the spin Hall effect of light inside semiconductors via absorption," *Opt. Lett.* **34**(15), 2312-2314 (2009).
7. X. Zhou, Z. Xiao, H. Luo, and S. Wen, "Experimental observation of the spin Hall effect of light on a nanometal film via weak measurements," *Phys. Rev. A* **85**(4), 043809 (2012).
8. N. Hermosa, A. M. Nugrowati, A. Aiello, and J. P. Woerdman, "Spin Hall effect of light in metallic reflection," *Opt. Lett.* **36**(16), 3200-3202 (2011).
9. Y. Qin, Y. Li, X. Feng, Y. F. Xiao, H. Yang, and Q. Gong, "Observation of the in-plane spin separation of light," *Opt. Express* **19**(10), 9636-9645 (2011).
10. C. C. Chan and T. Tamir, "Angular shift of a Gaussian beam reflected near the Brewster angle," *Opt. Lett.* **10**(8), 378-380 (1985).
11. M. Merano, A. Aiello, M. P. van Exter, and J. P. Woerdman, "Observing angular deviations in the specular reflection of a light beam," *Nature Photon.* **3**(6), 337-340 (2009).
12. M. Merano, N. Hermosa, A. Aiello, and J. P. Woerdman, "Demonstration of a quasi-scalar angular Goos-Hänchen effect," *Opt. Lett.* **35**(21), 3562-3564 (2010).
13. C. Leyder, M. Romanelli, J. Ph. Karr, E. Giacobino, T. C. H. Liew, M. M. Glazov, A. V. Kavokin, G. Malpuech, and A. Bramati, "Observation of the optical spin Hall effect," *Nature Phys.* **3**, 628-631 (2007).
14. Y. Gorodetski, K. Y. Bliokh, B. Stein, C. Genet, N. Shitrit, V. Kleiner, E. Hasman, and T. W. Ebbesen, "Weak Measurements of Light Chirality with a Plasmonic Slit," arXiv: 1204. 0378v2.
15. Y. Aharonov, D. Z. Albert, and L. Vaidman, "How the result of a measurement of a component of the spin of a spin -1/2 particle can turn out to be 100," *Phys. Rev. Lett.* **60**(14), 1351-1354 (1988).

16. H. Luo, X. Zhou, W. Shu, S. Wen, and D. Fan, "Enhanced and switchable spin Hall effect of light near the Brewster angle on reflection," *Phys. Rev. A* **84**(4), 043806 (2011).

17. N. Hermosa, M. Merano, A. Aiello, and J. P. Woerdman, "Orbital angular momentum induced beam shifts," *Proc. SPIE* **7950**, 79500F (2011).

18. N. Hermosa, A. Aiello, and J. P. Woerdman, "Radial mode dependence of optical beam shifts," *Opt. Lett.* **37**(6), 1044-1046 (2012).

19. H. Luo, X. Ling, X. Zhou, W. Shu, S. Wen, and D. Fan, "Enhancing or suppressing the spin Hall effect of light in layered nanostructures," *Phys. Rev. A* **84**(3), 033801 (2011).

1. Introduction

The spin Hall effect (SHE) of light manifests itself as a transverse spin-dependent splitting, when a spatially confined light beam passes from one material to another with different refractive index [1,2]. Recently, the transverse splitting has been reported at an air-prism interface via weak measurements [3–5]. On an air-semiconductor interface, the transverse splitting has been detected via ultrafast pump-probe techniques [6]. At an air-metal interface, the transverse splitting has been reported for the use of weak measurements and lock-in amplifying methods [7,8]. More recently, an in-plane spin-dependent splitting has been observed when a linearly polarized Gaussian beam impinges upon an air-prism interface [9]. The spin-dependent splitting is generally believed as a result of an effective spin-orbital coupling known as the influence of the intrinsic spin (polarization) on the trajectory, which produces transverse deflection of the spin. However, among these systems, the spin-dependent splitting is tiny and reaches just a fraction of the wavelength, limiting its future application.

In the present paper, we reveal a large spin angular splitting when a slightly elliptical polarization beam incidents at the Brewster angle. The reflected beam splits into two beams with opposite spin polarizations propagating at different angles. As a result, we can angularly separate the beam with different polarizations. It should be mentioned that the angular splitting is significantly different from that in previous works where the splitting is limited to the light intensity [10–12]. As an analogy of SHE in semiconductor microcavity [13], the directions of spin accumulations can be switched by adjusting the initial handedness of polarization.

Importantly, this large spin angular splitting is explored with an interesting simple weak measurements system which is similar to that of Ref. [14]. They propose that the coupling of a tightly focused optical beam to surface plasmon polaritons offers a natural weak measurements tool with a built-in post-selection. In our work, the combination of the slightly elliptical polarization incident beam with the reflected light beam at the Brewster angle also provides a built-in post-selection weak measurements technique for us. This simple weak measurements method shows significant difference from the previous works in which an additional post-selection is needed [3,4,15]. This spin angular splitting is also different from our previous work [16] where a linear polarization light beam incidents near the Brewster angle and a large spatial shift is observed. In addition, our work should be distinguished from the angular Imbert-Fedorov shift [17,18] whose angular splitting is in the orthogonal plane of incidence.

2. Theoretical analysis

The spin angular splitting is schematically shown in Fig. 1(a). The z -axis of the laboratory Cartesian frame (x, y, z) is normal to the air-prism interface. We use the coordinate frames (x_i, y_i, z_i) and (x_r, y_r, z_r) to denote incidence and reflection, respectively. A left- or right-elliptically polarized light beam incidents at the air-prism interface. Here, we choose the long and short axis of the elliptical polarization beam along to the x_i - and y_i -axis, respectively. The elliptical polarization light beam can be decomposed into two orthogonal polarization components H and V . It is noted that the mechanism of the elliptical polarization beam reflection on the prism at the Brewster angle acts as a built-in post-selection in which the H component is

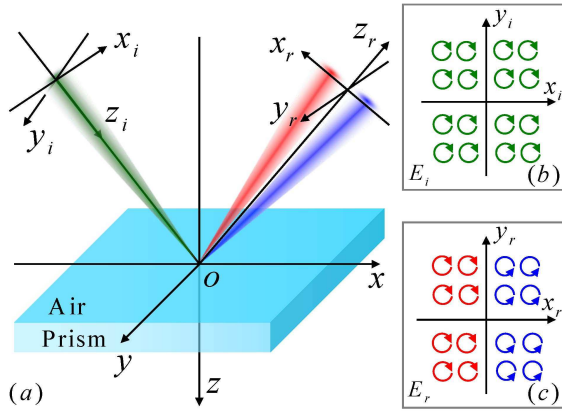


Fig. 1. (a) Schematic illustrating the spin angular splitting compared to the geometrical-optics prediction. (b) The incident beam has an uniform polarization direction in the cross section. (c) The polarization handedness experience different rotations in reflection to satisfy transversality.

mainly cut off and is equal to the V component. That is to say, this mechanism takes the role of the second polarizer in the precious weak measurements technique. After reflection, the H and V components overlap and induce the large spin angular splitting. Additionally, the reflection coefficient of H polarization component changes its sign across the Brewster angle, which means the induced total circular polarization reverses its handedness [Fig. 1(b) and 1(c)]. In other words, the two reflected beams are "colored" by different circular polarization. Selection of circular polarization in these beams is the post-selection procedure in the weak-measurement technique.

We theoretically analyze the spin angular splitting with a general beam propagation model. The reflected field $\tilde{\mathbf{E}}_r$ is related to the incident angular spectrum $\tilde{\mathbf{E}}_i$ by means of the relation [2, 19]

$$\begin{bmatrix} \tilde{\mathbf{E}}_r^H \\ \tilde{\mathbf{E}}_r^V \end{bmatrix} = \begin{bmatrix} r_p & \frac{k_{ry}(r_p+r_s)\cot\theta_i}{k_0} \\ -\frac{k_{ry}(r_p+r_s)\cot\theta_i}{k_0} & r_s \end{bmatrix} \begin{bmatrix} \tilde{\mathbf{E}}_i^H \\ \tilde{\mathbf{E}}_i^V \end{bmatrix}. \quad (1)$$

Here, H and V represent horizontal and vertical polarization components, respectively. θ_i is the incident angle, r_p and r_s denote the Fresnel reflection coefficients for parallel and perpendicular polarizations, respectively. k_0 is the wave number in free space.

In the spin basis set, the incident angular spectrum for H and V polarizations can be written as: $\tilde{\mathbf{E}}_i^H = (\tilde{\mathbf{E}}_{i+} + \tilde{\mathbf{E}}_{i-})/\sqrt{2}$ and $\tilde{\mathbf{E}}_i^V = i(\tilde{\mathbf{E}}_{i-} - \tilde{\mathbf{E}}_{i+})/\sqrt{2}$. Here, $\tilde{\mathbf{E}}_{i+} = (\mathbf{e}_{ix} + i\mathbf{e}_{iy})\tilde{\mathbf{E}}_i/\sqrt{2}$ and $\tilde{\mathbf{E}}_{i-} = (\mathbf{e}_{ix} - i\mathbf{e}_{iy})\tilde{\mathbf{E}}_i/\sqrt{2}$ denote the left- and right-circular polarized (spin) components, respectively. We consider the incident beam with a Gaussian distribution and its angular spectrum can be written as

$$\tilde{\mathbf{E}}_i = \frac{w_0}{\sqrt{2\pi}} \exp\left[-\frac{w_0^2(k_{ix}^2 + k_{iy}^2)}{4}\right], \quad (2)$$

where w_0 is the beam waist. The reflected angular spectrum can be obtained from Eq. (1). In the spin basis, $\tilde{\mathbf{E}}_r^H = (\tilde{\mathbf{E}}_{r+} + \tilde{\mathbf{E}}_{r-})/\sqrt{2}$, $\tilde{\mathbf{E}}_r^V = i(\tilde{\mathbf{E}}_{r-} - \tilde{\mathbf{E}}_{r+})/\sqrt{2}$. Here, $\tilde{\mathbf{E}}_{r+} = (\mathbf{e}_{rx} + i\mathbf{e}_{ry})\tilde{\mathbf{E}}_r/\sqrt{2}$ and $\tilde{\mathbf{E}}_{r-} = (\mathbf{e}_{rx} - i\mathbf{e}_{ry})\tilde{\mathbf{E}}_r/\sqrt{2}$, where $\tilde{\mathbf{E}}_r$ can be obtained from the boundary conditions: $k_{ix} = -k_{rx}$ and $k_{iy} = k_{ry}$.

As for the elliptical polarization incident light beam, the Jones vector can be written as $(\cos\Delta, e^{i\varphi} \sin\Delta)^T$. Here Δ represents the azimuth angle (the angle between the crystal axis of wave plate and the x_i -axis) and φ denotes the phase difference between the two polarization components H and V . In the present study, we consider a elliptical polarization beam with its long and short axis along to the x_i - and y_i -axis. Therefore the Jones vector will be simplified to $(\cos\Delta, +i \sin\Delta)^T$ or $(\cos\Delta, -i \sin\Delta)^T$ representing the left- or right-elliptical polarization in the case of angle $\varphi = \pm\pi/2$. And we note here that the azimuth angle Δ mentioned in the following is a tiny value allowing for a slightly elliptical polarization and its long axis along to the x_i -axis.

We firstly take left-elliptical polarization incident light beam as an example and the right-elliptical polarization can be obtained in the similar way. The Jones vector of the left-elliptical polarization is $(\cos\Delta, i \sin\Delta)^T$. Therefore, according to Eqs. (1) and (2), we can obtain the reflected angular spectrum:

$$\tilde{\mathbf{E}}_r = \frac{r_p \cos\Delta}{\sqrt{2}} [(1 + i \tan\Delta k_{ry} \delta_{ry} + \eta) \tilde{\mathbf{E}}_{r+} + (1 + i \tan\Delta k_{ry} \delta_{ry} - \eta) \tilde{\mathbf{E}}_{r-}]. \quad (3)$$

Here, $\delta_{ry} = (1 + r_s/r_p) \cot\theta_i/k_0$ and $\eta = ik_{ry}\delta_{ry} + r_s \tan\Delta/r_p$. At any given plane $z_r = \text{const.}$, the transverse displacement of field centroid compared to the geometrical-optics prediction is given by

$$\delta_{\pm} = \frac{\iint \tilde{\xi}_{r\pm}^* i \partial_{k_{rx}} \tilde{\xi}_{r\pm} dk_{rx} dk_{ry}}{\iint \tilde{\xi}_{r\pm}^* \tilde{\xi}_{r\pm} dk_{rx} dk_{ry}}, \quad (4)$$

where $\tilde{\xi}_{r\pm} = r_p \cos\Delta (1 + i \tan\Delta k_{ry} \delta_{ry} \pm \eta) \tilde{\mathbf{E}}_{r\pm}$. We note that there needs a theoretical correction and the higher-order terms should be taken into account when the beam is incident near the Brewster angle [16]. By making use of a Taylor series expansion based on the arbitrary angular

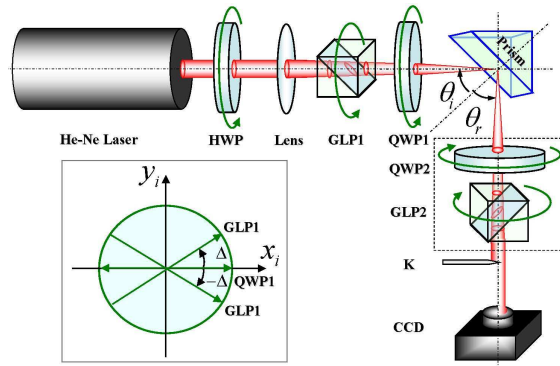


Fig. 2. (a) Experimental setup for characterizing the large spin angular splitting on reflection at the Brewster angle. The light source is a 17mW linearly polarized He-Ne laser at 632.8nm (Thorlabs HRP170); Prism with refractive index $n = 1.515$ (BK7 at 632.8nm); Lens, lens with effective focal length: 50mm; HWP, half-wave plate (for adjusting the intensity); QWP1 and QWP2, quarter-wave plates; GLP1 and GLP2, Glan Laser polarizers; Here, QWP2 together with GLP2 allow for measuring the Stokes parameter S_3 ; K, knife edge (The purpose of the knife is to produce a single spin accumulation so that only one spin component can be detected in the CCD); CCD, charge-coupled device (Coherent LaserCam HR). The inset: The incident beam is preselected in the left- or right-elliptical polarization state by GLP1 whose optical axis make angles Δ or $(-\Delta)$ with x_i -axis. Here, we choose $\Delta=0.5^\circ$.

spectrum component, r_p and r_s can be expanded as a polynomial of k_{ix} :

$$r_{p,s}(k_{ix}) = r_{p,s}(k_{ix} = 0) + k_{ix} \left[\frac{\partial r_{p,s}(k_{ix})}{\partial k_{ix}} \right]_{k_{ix}=0} + \sum_{j=2}^N \frac{k_{ix}^N}{j!} \left[\frac{\partial^j r_{p,s}(k_{ix})}{\partial k_{ix}^j} \right]_{k_{ix}=0}. \quad (5)$$

Using this method, we can obtain the theoretical shift of the single circular polarization component induced by angular splitting in the case of left-elliptical polarization:

$$\delta_{\pm} = \pm \frac{2z_r r_s \frac{\partial r_p}{\partial \theta_i} [(k_0 R + \csc^2 \theta_i - 1) \sin 2\Delta + \csc^2 \theta_i - 1]}{k_0 R [2k_0 R r_s^2 - (\frac{\partial r_p}{\partial \theta_i})^2] \cos 2\Delta - [2k_0 R r_s^2 + (\frac{\partial r_p}{\partial \theta_i})^2] (k_0 R + \csc^2 \theta_i + \cot^2 \theta_i \sin 2\Delta - 1)}. \quad (6)$$

Here $R = k_0 w_0^2 / 2$, w_0 is the beam waist and z_r is the propagation distance. It should be noted that the reflected light beam will experience a spatial shift in the case of linear polarization and a angular displacement according to the elliptical polarization. In this work, we only consider the elliptical polarization in which the large spin angular splitting is explored.

3. Weak measurements system

Next, we focus our attention on the experiment. Figure 2 illustrates the experimental setup. A Gaussian beam generated by a He-Ne laser is preselected as a slightly elliptical polarization state by GLP1 and QWP1. By choosing the focal length of lens, we can obtain the desired beam waist in reflection. When the beam impinges onto the prism interface, the reflected beam is angularly separated into two opposite spin components. The prism is mounted to a rotation stage allowing for precise control of the incidence at the Brewster angle. It should be noted that the reflected mechanism discussed above can be seen as a built-in post-selection amplified technique in which the angular splitting is significantly amplified. To detect the angular splitting, a knife edge is applied to achieve a distribution of single spin component. We use a CCD to measure the centroid of the spin accumulation after the knife edge. Using additional QWP2 and GLP2, we can measure the Stokes parameter S_3 which reveals the circular polarization state of the angular splitting [13].

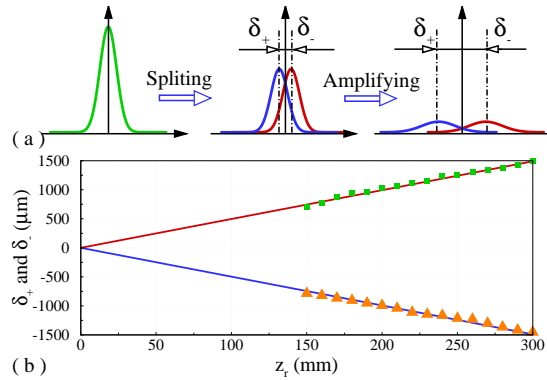


Fig. 3. (a) Preselection and postselection of polarizations give rise to an amplified spin angular splitting. (b) Theoretical and experimental results of two spin components induced by the spin angular splitting for beam waist $w_0 = 18.66 \mu\text{m}$. We measured the z_r from the beam waist. The incident light beam is left-elliptical polarization for $\Delta=0.5^\circ$ from the x_i -axis and incidents at the Brewster angle $\theta_i = 56.57^\circ$.

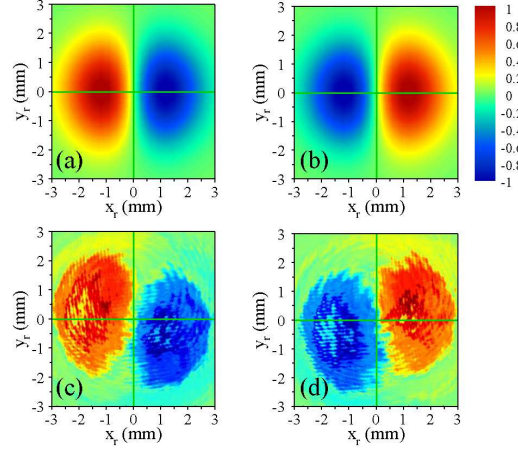


Fig. 4. Theoretical and experimental results of Stokes parameter S_3 : (a), (b) Theoretical calculation of Stokes parameter S_3 for the left- and right-elliptical polarization; (c), (d) Experimental results concluded from the intensity distributions on CCD. The directions of the spin accumulation can be switched by adjusting the initial handedness of polarizations. Here, the parameters are the same as that of Fig. 3. The distributions in the plane $z_r = 300\text{mm}$ are plotted with normalized units.

The amplifying mechanism of spin angular splitting is schematically shown in Fig. 3(a). The incident beam is preselected in the elliptical polarization, and then postselected in the circular polarization state when it reflects on the prism at the Brewster angle. In our measurement, we first choose the lens with focal length $f = 50\text{mm}$ to generate beam waist $w_0 = 18.66\mu\text{m}$ and make the incident light beam at the Brewster angle by modulating the GLP1 along to the x_i -axis. Then we select the incident light beam as slightly left-elliptical polarization by modulating the $\Delta=0.5^\circ$ from the x_i -axis. Limited by the large holders of the knife edge and diaphragm, the angular splitting at small propagation distance are not measured. We measure the displacements every 10mm from 150mm to 300mm [Fig. 3(b)]. The detected splitting value reaches about $1500\mu\text{m}$ at the plane of $z_r = 300\text{mm}$. The solid lines represent the theoretical predictions. The experimental results are in good agreement with the theory without using parameter fit.

To obtain a clear physical picture, it is necessary to analyze the polarization distribution of the reflected light beam. The Stokes parameter S_3 is introduced to describe the circular polarization state of the spin angular splitting. Here, $S_3=+1$ or -1 represents the left- or right-circular polarization. Figure 4(a) and 4(b) illustrate the theoretical polarization distribution of reflected light beam considering the different left- and right-elliptical polarization incident beam. We can clearly see that, with the incident beam elliptical polarization state changing from left (right) to right (left), the spin angular splitting will reverse the direction. As an analogy of SHE in electronic system [13], the directions of spin accumulations can be switched by the initial handedness of polarization.

We also carry out another experiment to measure the polarization distribution described by Stokes parameter S_3 . The experimental setup is similar to the first experiment. A new Glan laser polarizer (GLP2) and a new quarter-wave plate (QWP2) are added behind the prism. The last Glan laser polarizer, quarter-wave plate and CCD establish a general experimental system for measuring polarization distribution. By rotating the GLP2 to two angles and holding the QWP2 along to the y_r -axis, we can conclude the Stokes parameter S_3 from the intensity distributions on CCD. The rotation angles are 45° and 135° , the deviations from the configuration of the

y_r -axis. The experimental results shown in Fig. 4(c) and 4(d) are in good agreement with the theoretical calculation.

4. Conclusions

In conclusion, we have revealed a large spin angular splitting on reflection at the Brewster angle. The detected splitting reaches about $1500\mu\text{m}$ at $z_r = 300\text{mm}$. As an analogy of SHE in semiconductor microcavity [13], we are able to switch the directions of the spin accumulations by adjusting the initial handedness of spin states. This phenomenon can be interpreted from the inversion of horizontal electric field vector across the Brewster angle. Importantly, we propose a simple weak measurements system offering an interesting built-in post-selection technique to explore this angular splitting, which will provide us a new method on weak measurements technique.

Acknowledgments

We are sincerely grateful to the anonymous referees, whose comments have led to a significant improvement of our paper. This research was partially supported by the National Natural Science Foundation of China (Grants Nos. 61025024 and 11074068).